Aseismic continuation of the Lesser Antilles slab beneath continental South America

J. C. VanDecar,[1,2] R. M. Russo,[3] D. E. James,[1] W. B. Ambeh,[4] and M. Franke[5]

Received 2 August 2001; revised 18 June 2002; accepted 22 October 2002; published 25 January 2003.

[1] We present results of travel time inversions of teleseismic *P* and *S* waves recorded at the SECaSA92 (Southeast Caribbean South America 1992) temporary broadband array in northeastern Venezuela and Trinidad. The inversions reveal the unusual structure of the southern termination of the Lesser Antilles subduction zone: A minimum 2% relatively high-velocity anomaly trends WSW from the seismically defined Lesser Antilles slab beneath and NW of the Paria Peninsula to a point below the Venezuelan Serranía del Interior, well south of the Caribbean coast. Resolution tests utilizing actual ray geometries and densities of the source data indicate that the regional-scale structure beneath the study area is reasonably well resolved. Thus a detached and detaching subducted South American slab appears to lie beneath continental South America. We infer that oceanic South American lithosphere has been overridden to a significant degree by continental South America. The detached slab now lying beneath continental South America was driven into its current position after detaching from the former eastward striking Mesozoic ocean-continent passive margin as this margin entered the subduction zone. Because oceanic and continental South America are still attached without apparent relative motion between them along the Atlantic passive margin southeast of our study region, the slab must be the actively moving element during continental overriding. Thus the slab and its surrounding mantle (both Caribbean and South America) beneath northeastern South America are mobile and have moved ESE relative to the stable Guyana Shield craton. *INDEX TERMS:* 7203 Seismology: Body wave propagation; 7218 Seismology: Lithosphere and upper mantle; 8120 Tectonophysics: Dynamics of lithosphere and mantle—general; 8180 Tectonophysics: Evolution of the Earth: Tomography; *KEYWORDS:* tomography, seismic structure, Venezuela, subduction, upper mantle, slab tearing

Citation: VanDecar, J. C., R. M. Russo, D. E. James, W. B. Ambeh, and M. Franke, Aseismic continuation of the Lesser Antilles slab beneath continental South America, *J. Geophys. Res.*, *108*(B1), 2043, doi:10.1029/2001JB000884, 2003.

1. Introduction

[2] The eastern Caribbean (Ca)-South America (SA) plate boundary zone (Figure 1) is characterized by complex geology [*Metz*, 1968; *Salvador and Stainforth*, 1968; *Schubert*, 1971; *Rossi et al.*, 1987; *Avé Lallement and Guth*, 1990; *Roure et al.*, 1994; *Parnaud et al.*, 1995; *Passalacqua et al.*, 1995; *Avé Lallement*, 1997], near superposition of active strike-slip and thrust seismic deformations [*Molnar and Sykes*, 1969; *Perez and Aggarwal*, 1981; *Russo et al.*, 1992, 1993] and a slow plate interaction velocity of 1–2 cm yr^{-1}, as determined from requirements of global plate velocity closure [*DeMets et al.*, 1990]. Surface geology in NE Venezuela and Trinidad reveals north-to-south juxtaposition of a meta-igneous oceanic crustal terrane exotic to South America, a metamorphosed accretionary wedge of South America derived sediments, and a wide foreland thrust belt (the Serranía) and foreland basin currently developed above Guyana Shield basement [*Bladier*, 1979; *Feo-Codecido et al.*, 1984; *Speed*, 1985; *Rossi et al.*, 1987; *Russo and Speed*, 1992, 1994]. These tectonic units are bounded by faults (Figure 1), which together with regional folding of sediments in the foreland deformation belt, are consistent in orientation with deformation in a wide dextral transpressive shear zone. There has been at least 70 km of north-south crustal shortening in the southeast vergent foreland thrust belt [*Rossi et al.*, 1987; *Passalacqua et al.*, 1995]. Southward transport of the metamorphosed coastal accretionary units is an important constraint on the northerly extent of continental South America: binary age protoliths of these metamorphosed sediments indicate that they are derived from the Guyana Shield and were deposited on South America's northern continental shelf before being thrust SE over the shelf into their present position [*Foland*

[1]Department of Terrestrial Magnetism, Carnegie Institution of Washington, Washington, D. C., USA.
[2]Also at Nature, London, UK.
[3]Department of Geological Sciences, Northwestern University, Evanston, Illinois, USA.
[4]Seismic Research Unit, University of the West Indies, St. Augustine, Trinidad, Trinidad and Tobago.
[5]Kinematics, Inc., Pasadena, California, USA.

0148-0227/03/2001JB000884$09.00

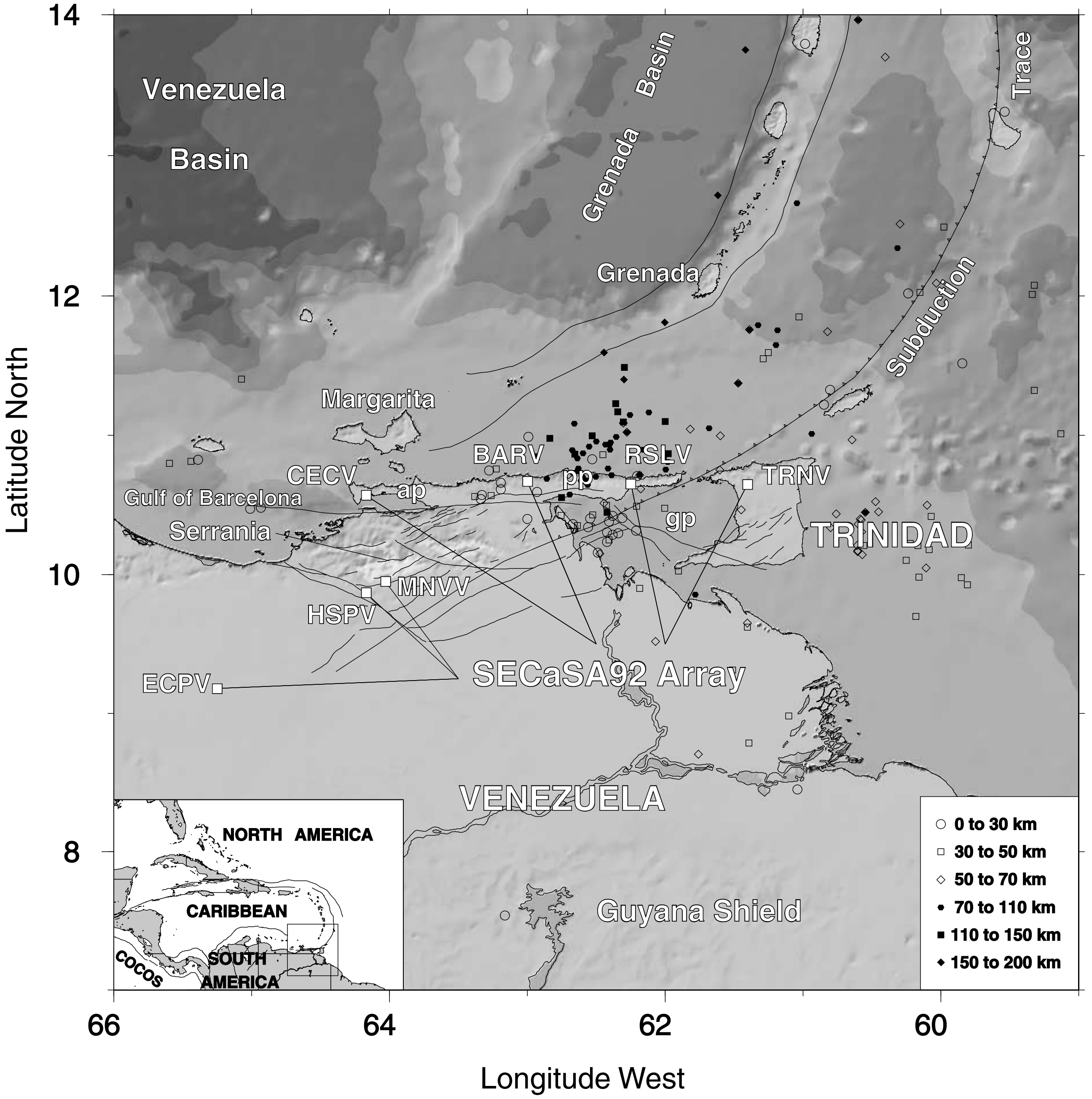

Figure 1. Map of study region. Coastlines (black) overlain on 2-min bathymetry [*Smith and Sandwell*, 1997] and topography (30-s NGDC). Boundaries of Lesser Antilles arc platform shown in black; lithospheric subduction trace is heavy white line, teeth on overriding side. Faults of the foreland region also shown (thin black lines). SECaSA92 station locations are white squares. Filled and unfilled black symbols are NEIC seismicity 1963–1993, 20 or more recording stations. Geographic place names: ap, Araya Peninsula; pp, Paria Peninsula; gp, Gulf of Paria; Serranía, Serranía del Interior. See color version of this figure at back of this issue.

et al., 1992]. Thus, continental South America extends beneath these units north of the present coastline [*Ysaccis and Bally*, 1997].

[3] Westward subduction of oceanic South America along the southern Lesser Antilles subduction zone is largely aseismic [*Wadge and Shepherd*, 1984], but sporadic intermediate depth seismicity indicates subducted oceanic South American plate exists to at least 200 km depth beneath the island arc [*Molnar and Sykes*, 1969; *Russo et al.*, 1992, 1993]. Intermediate depth seismicity increases dramatically south of Grenada, and lies in a NE-SW trending linear region culminating at the Paria Peninsula of NE Venezuela (Figure 1). Shallow (0–70 km) seismicity in the vicinity of Paria is patchy and indicates complex surface motions but a cluster of more frequent intermediate depth (70–200 km) events define a steeply dipping subducted slab beneath the

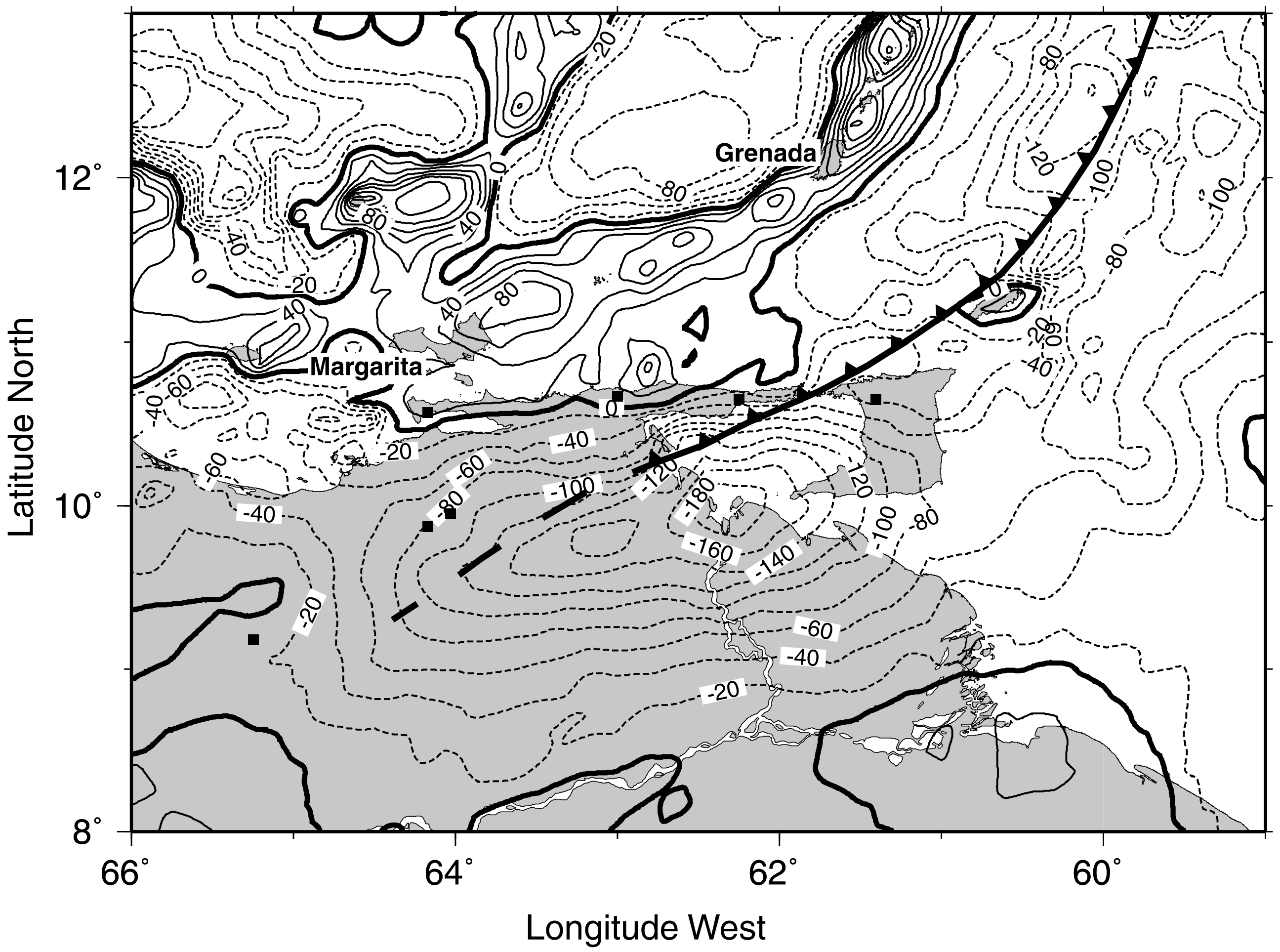

Figure 2. Free-air gravity anomalies of study region [after *Russo and Speed*, 1994]. Solid lines are positive anomaly contours, dashed lines are negative anomaly contours; contour interval is 20 mGal. Lithospheric subduction trace also shown (black). Note continuity of high gravity anomalies of the Lesser Antilles arc platform between Grenada and Margarita. Large negative SE anomaly, centered on western coast of Gulf of Paria is roughly parallel to arc platform as defined by gravity. CaSA92 stations are black squares.

Paria Peninsula (Figure 1) [*Perez and Aggarwal*, 1981; *Russo et al.*, 1993]. This slab is continuous along strike with oceanic South America subducting along the Lesser Antilles further north [*Van der Hilst*, 1990; *Russo et al.*, 1992, 1993]. However, intermediate-depth seismicity, which defines the slab, ceases abruptly beneath the western Gulf of Paria.

[4] Recent volcanic arc activity has not been observed south of Grenada (12°N; Figure 2), although gravity and magnetic anomalies associated with the volcanic arc platform continue in the local strike direction of the arc, trending WSW from Grenada to Margarita [*Speed et al.*, 1984; *Russo and Speed*, 1994]. The southwestward extension of the arc platform is parallel to and north of the Paria slab. South of the slab, a pronounced Bouguer gravity minimum of nearly −200 mGal [*Bonini*, 1978; *Russo and Speed*, 1994] crosses the Gulf of Paria between Trinidad and Venezuela and extends WSW inland (this represents the world's lowest continental Bouguer gravity anomaly found at sea level). The negative gravity anomaly is roughly parallel to the arc platform extension, forming a positive-negative gravity pair characteristic of subduction zones. The subducting slab, as defined by the spatial extent of seismicity, parallels both anomalies and lies between them, but it does not extend west of Paria, as does the gravity anomaly pair. This large negative Bouguer gravity anomaly and its existence at sea level is most likely indicative of a very large load on South American lithosphere here (discussed further below) [*Russo and Speed*, 1992].

[5] We show in this paper that subducted aseismic South American oceanic lithosphere lies under northern Venezuela, beneath continental South America, extending along a SW trend 150–200 km from the end of the seismically defined slab beneath Paria to a point near the western edge of the Venezuelan Serranía (approximately 9°N, 65.5°W). Our result is largely consistent with the tomography results of *Van der Hilst* [1990] and *Bosch* [1997] and with the analysis of *Russo and Speed* [1992] regarding tectonic wedging of South American continental lithosphere between overriding Caribbean terranes and underthrust South American oceanic slab. The load this slab places on the lithosphere accounts for the large negative gravity anomalies over the Venezuelan foreland by downwarping

South American continental lithosphere and displacement of the mantle below, a suggestion also made by *Van der Hilst* [1990]. The slab apparently detaches from the surface lithosphere beneath Paria concentrating seismic strain there, whereas stresses in the detached slab are released and the slab sinks aseismically in mechanical equilibrium beneath South America. Overriding of the slab by the continent is a clear indication that the mantle beneath the former north-facing South American passive margin was mobilized during Ca-SA plate interaction [*Russo et al.*, 1996].

2. SECaSA92 Array and Data Set

[6] The SECaSA92 temporary broadband seismic array was deployed in NE Venezuela and Trinidad from May 1992 to October 1993. The goal of the deployment was to characterize the southern termination of the Lesser Antilles subduction zone. Six seismometers were placed at seven sites (one station was moved during the experiment) parallel to and across the Ca-SA plate boundary zone (Figure 1). Four stations (TRNV, RSLV, BARV, and CECV) were situated along the northern coasts of Venezuela and Trinidad, crossing the Paria intermediate depth seismicity at high angle. Three sites (BARV, MNVV-HSPV, and ECPV) formed a line parallel to the local NE strike of the Paria cluster seismicity and extending SW of the coast across the foreland deformation belt and well into the Venezuelan Llanos basin. Station spacing was approximately 100 km. The seismometers were placed in specially built concrete vaults on concrete pads approximately 1 m below ground level. We used Reftek data loggers in conjunction with Omega navigation signals to achieve absolute timing to 1 ms accuracy.

3. Inversion for Upper Mantle Structure

[7] We determined relative arrival times of compressional (*P*) and shear (*S*) waves recorded at the SECaSA92 array via a multichannel cross-correlation procedure that makes use of the duplicate information obtained by cross-correlating all possible pairs of waveforms [*VanDecar and Crosson*, 1990]. This procedure produces both highly accurate delay times (standard errors of approximately 0.03 s for *P* waves and 0.10 s for *S* waves) and useful standard error estimates. Each event was individually analyzed with various filter and cross-correlation settings to test for consistency and to ensure against cycle skipping and biases induced by waveform distortion. In order to guard against timing errors due to phase misidentification or multiple phase interference, we generated and processed WKBJ synthetic seismograms [*Aki and Richards*, 1980] in parallel with the data whenever source-receiver geometries indicated the possibility of simultaneous phase arrival at the array. We assume that the infinite frequency approximation is valid, and thus the energy from earthquake to seismometer travels solely along a ray path. This approximation is useful when material properties are varying slowly with respect to the wavelength of the seismic wave. For our study, wavelengths are about 8 km for *P* waves and 35 km for *S* waves, whereas the smallest structures that we image have wavelengths of around 100 km. We also assume that our initial guess at earthquake locations and ray paths are relatively close to the real locations (within the linear approximation) or that by iteratively performing linear inversions we will reach this point. To minimize nonlinear effects, we used only earthquakes at teleseismic distances ($\Delta > 30°$) [*Neele et al.*, 1993a] so as to avoid ambiguities that arise owing to the waveform triplications that affect rays bottoming within the mantle transition zone.

[8] We parameterize variations in Earth structure beneath our stations with splines under tension constrained at a series of regular knots [*Cline*, 1981; *Neele et al.*, 1993b], which allows us both smooth slowness variations, advantageous for ray tracing through the resulting models, and also relatively local structure (compared to cubic splines which have large side lobes). We use 32 knots in depth, 29 in latitude and 37 in longitude for a total of 34,336 knots parameterizing perturbation in slowness. The grid extends from 0 to 1000 km in depth, 5 to 15°N in latitude, and 57 to 69°W in longitude. Within the interior portion of the model (0–400 km depth, 9–12°N, 60–67°W), the knots are spaced 25 km apart in depth and 1/4 degree apart in latitude and longitude, allowing us to resolve structure with about a 50-km spatial wavelength. We obtain the best resolution in this portion of the model. We include knots in the exterior region to mitigate against the mapping of unwarranted and spurious structure in regions outside our model [*Neele et al.*, 1993a, 1993b].

[9] We inverted *P* and *S* wave relative arrival times independently for compressional- and shear wave slowness (1/velocity) perturbations. For each, we invert simultaneously for slowness, earthquake relocations, and station terms. Although our data set is not highly dependent on earthquake location, earthquake mislocation or heterogeneous structure far from our study area will induce a trend in time across the network. Although these trends are not constant between events, and therefore are not much mapped into structure, if unaccounted for they do bias our estimates of variance reduction used to construct pseudo-variance/resolution trade-off plots. The station terms (which are calculated taking into account variations in ray arrival angles) are necessary to account for shallow crustal heterogeneity as well as differences in station elevations. The distributions of events used in this study (25 associated with *P* wave and 44 *S* wave data) provide reasonable azimuthal coverage with respect to the network. Locations of events with lower mantle turning points, relative to the array, are shown in Figure 3. We also used *P* and *S wave* core-phase arrivals (e.g., *PKP*, *SKS*) from six and eight events, respectively, to include ray paths that impinged nearly vertically upon the network. We made four or five arrival time observations for each event, leading to a total of 113 *P* wave and 194 *S* wave relative times to be inverted. Note that the events are reasonably well distributed with respect to azimuth from the network. This is important, since the degree to which we have rays crossing through a region determines how well we can resolve structure there.

[10] The linear system to be inverted is underdetermined (all parameters are not uniquely determined by the data), and thus we must add a priori information in order to obtain a unique solution or set of solutions. We invert by searching for the simplest model necessary, that is, the model containing the least amount of structure required to satisfy the observations to within their estimated standard errors [*Constable et al.*, 1987; *Neele et al.*, 1993b; *VanDecar and Snieder*, 1994; *Parker*, 1994; *Bostock and VanDecar*, 1995].

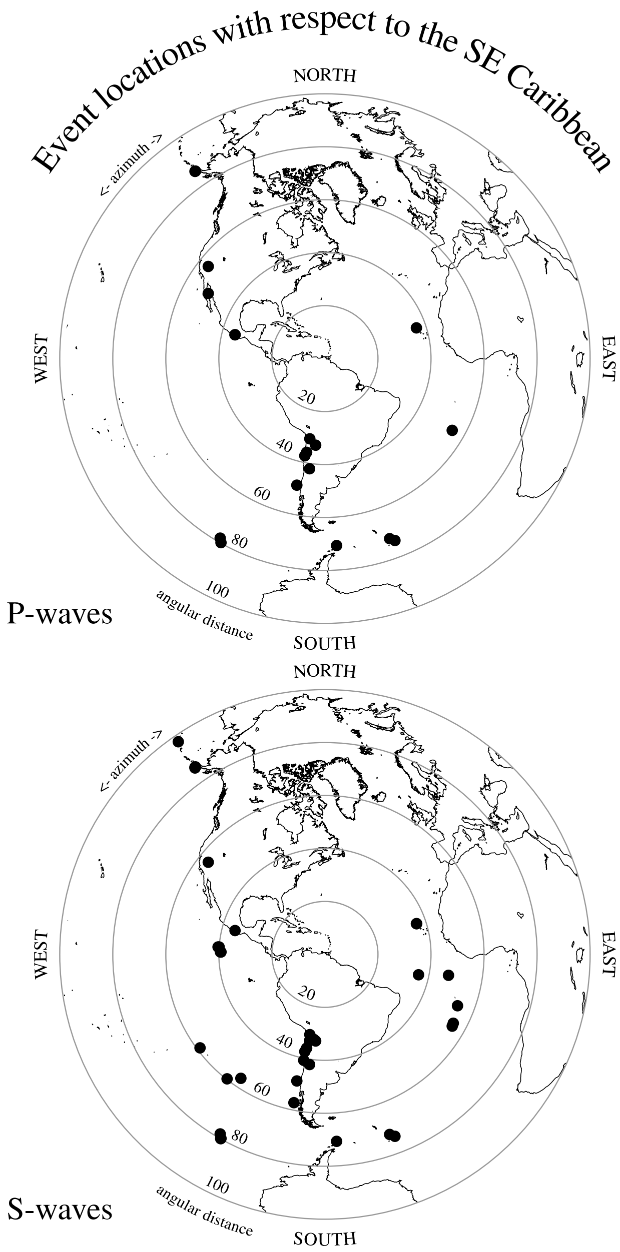

Figure 3. Locations relative to array of events with lower mantle bottoming rays (30°–98° Δ). Nineteen events from which *P* wave observations were used (top) and 36 events from which *S* wave observations were made (bottom). Four or five arrival times were determined at the array for each event. Note that we also used *P* and *S* core phases from six and eight events, respectively (not shown). A total of 113 *P* and 194 *S* wave observations were made.

Here we define "structure" by model derivatives and seek to equally minimize spatial gradients and roughness, implemented numerically through first- and second-difference operators. We invert these large linear systems with a conjugate gradients procedure iterated to convergence [*VanDecar and Snieder*, 1994]. We also iterate upon these inversions, systematically downweighting equations associated with outlying residuals from the previous iteration [*Bostock and VanDecar*, 1995]. The effect of this is to produce a robust solution with L2 (least squares) residual minimization within 1.5 residual standard deviations and, in the limit of many iterations, L1 (median) minimization for those equations associated with larger residuals [*Huber*, 1981]. We perform 20 iterations of the robust downweighting, and 2000 conjugate gradient iterations for each of these inversions. Thus, our models, even before robust downweighting, explain 95% of the root-mean square data residual for *P wave* data (from 0.82 to 0.04 s) and 90% for *S* wave data (from 1.43 to 0.14 s), in keeping with our a priori estimates of data error.

4. Slab Structure Beneath South America

[11] We show the results of our travel time inversion in Figure 4 as a series of three horizontal slices and a vertical section of contoured *P* and *S* wave per cent velocity perturbation. For both *P* and *S* wave models, we resolve a single structure, a tabular high-velocity (2–3% fast) anomaly striking NE and dipping approximately 60°NW. This structure is seen at 100, 200, and 300 km below the study region and maintains its tabular character throughout the high-resolution volume. The top and bottom of the anomaly are not well defined, but the top appears to lie between 50 and 150 km depth; the anomaly has no bottom within the high-resolution volume and extends to at least 400 km.

[12] To the NE, the anomaly is coincident with the southern end of the Lesser Antilles slab defined by earthquakes beneath the Paria Peninsula. Therefore, we can confidently identify the high-velocity anomaly with the subducting slab. However, the high-velocity anomaly extends 150–200 km SW of intermediate depth Paria seismicity. Because of its spatial association with the seismically active slab, and because of its along-strike continuity, we infer that the SW extension of the high-velocity anomaly is an aseismic portion of the oceanic South America slab. Thus, the slab appears to extend to a point approximately beneath the southwestern limit of the deformed foreland belt (Figure 1). This subducted lithosphere lies far SW of the Caribbean coast, and by inference lies below South American continental lithosphere. Subducted oceanic slab therefore lies beneath the metamorphic coastal terranes and the foreland deformation belt, largely consistent with the analysis of *Russo and Speed* [1992] and with the larger scale *P* wave delay-time tomographies of *Van der Hilst* [1990] and *Bosch* [1997].

[13] Our travel time inversion results for *P* and *S* wave velocity anomalies allow for an important refinement of *Van der Hilst*'s [1990] finding and of the *Russo and Speed* [1992] tectonic wedging model: the slab we find terminates further to the northwest of the proposed aseismic slab extension based on *Van der Hilst*'s [1990] results. We note that station ECPV lies southwest of the high-velocity anomaly along strike, and so we should have an accurate estimate of the anomaly's southwestern extent. Therefore, the aseismic slab terminates approximately beneath the juxtaposition of the deformed foreland belt with a more westerly portion of the foreland basin (Anaco Basin). *Van der Hilst* [1990] and *Russo and Speed* [1992, 1994] inferred that the aseismic slab extended some 500–700 km SW of Paria to a point at 7°N due south of Caracas, Venezuela. This does not appear to be the case, based on our travel time inversion of data collected in situ. *Van der Hilst and Mann* [1994] interpret

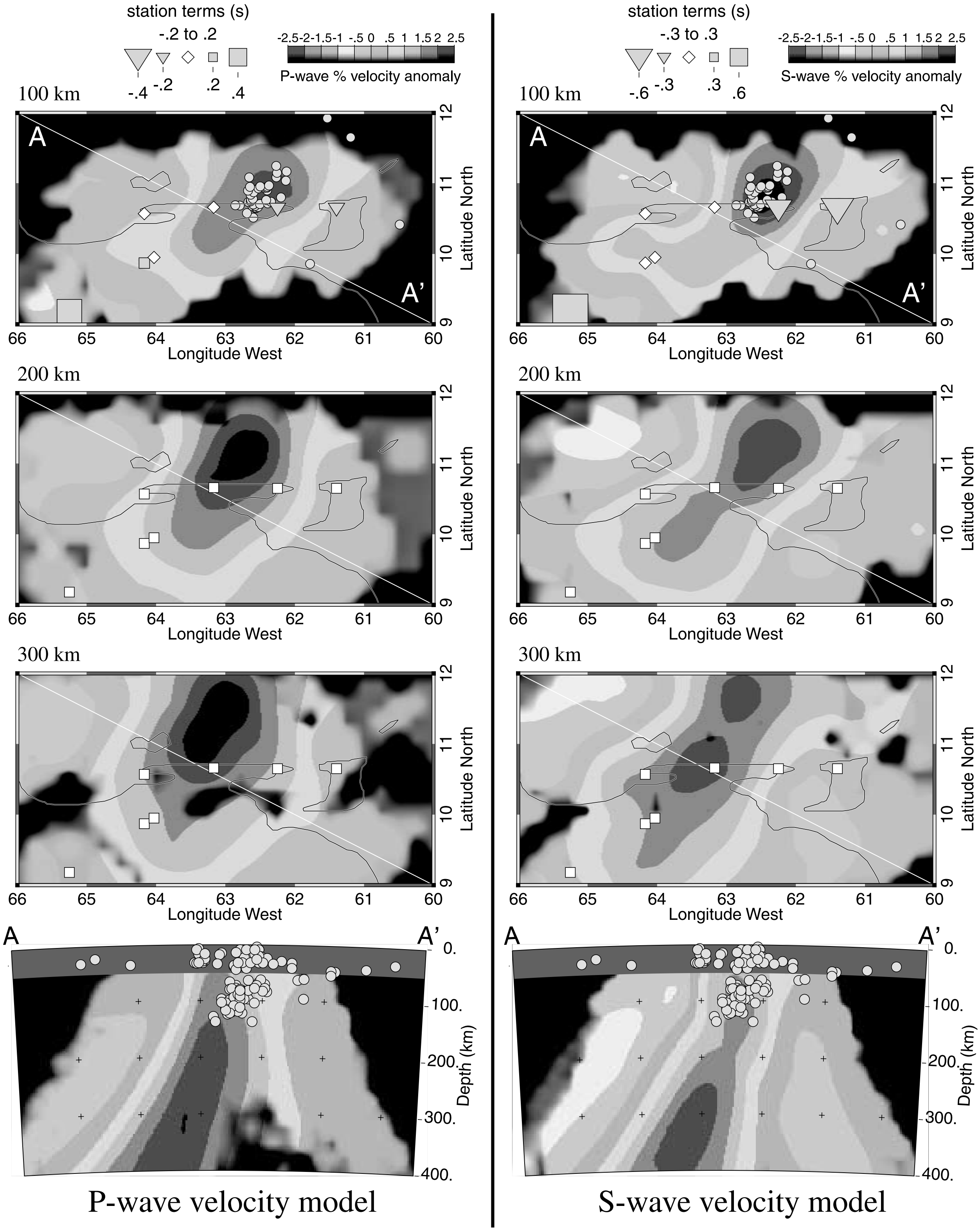

Figure 4. Horizontal sections through *P* wave (left) and *S* wave (right) velocity percent perturbation models (slowness, 1/velocity, was actually determined in the inversion) at constant depths of 100, 200 and 300 km; vertical cross sections (bottom) at locations shown by white lines in top three sections. Perturbations are with respect to global radial-Earth velocity model IASP91 [*Kennett and Engdahl*, 1991]. Yellow dots: earthquakes within ±30 km of each depth section. Note tabular high-velocity anomaly coincident with Paria slab earthquakes but extending SW from Paria beneath SA. We interpret this anomaly as both the seismically active and aseismic slab continuation beneath SA. See color version of this figure at back of this issue.

the high-velocity anomaly observed in this region as the downdip end of Caribbean lithosphere subducted beneath the Venezuelan Andes. Thus, there would appear to be two slabs beneath northern South America: the Lesser Antilles slab which we resolve here and a southward dipping slab of Caribbean lithosphere outside of our study area.

[14] Termination of the aseismic slab beneath the western limit of the foreland deformed belt leaves an interesting problem to consider. The Ca-SA plate interaction has proceeded diachronously, developing in time from west to east [*Speed*, 1985; *Russo and Speed*, 1992; *Passalacqua et al.*, 1995], consistent with long-term eastward motion of the Caribbean plate relative to a Pacific basin source [*Molnar and Sykes*, 1969]. The slab we observe is currently attached to continental South America east of Paria, and was attached to the continent north of the coast west of Paria before it was subducted and overridden by the continent. The slab we observe, if restored to its attached position would extend from Paria to approximately the eastern Gulf of Barcelona (Figure 1). If, as we observe, the slab ends abruptly along strike, then what lithosphere lay west of the slab when the latter was still at the surface? And where is that lithosphere now? If it subducted beneath the Caribbean, it must have been soon widely separated from the slab we observe for it is not within our study region. One possible answer to this question is that more westerly portions of subducted South American oceanic lithosphere have already sunk into the lower mantle where they may contribute to known high-velocity anomalies deep below the Caribbean Basin [*Jordan and Lynn*, 1974; *Jordan*, 1975; *Lay*, 1983; *Van der Hilst and Spakman*, 1989; *Grand*, 1994; *Kendall and Silver*, 1996].

5. Resolution Tests

[15] In order to ensure that the travel time inversion yields robust velocity structure beneath the study area, we performed various resolution tests, some of which are summarized in Figures 5 and 6. The tests consisted of incorporating a "synthetic" velocity anomaly of shape similar to that of the tabular slab structure determined through the travel time inversion of real data, with peak velocity perturbations of 5% with respect to surrounding upper mantle velocities. Then, given the actual ray geometries determined from 3D ray tracing through the synthetic slab models with the same seismic sources and station locations (with the addition of random Gaussian noise of 0.05 s RMS for the *P* wave and 0.1 s RMS for the *S* wave data), we determined the degree to which such structure was recovered by application of the nonlinear travel time inversion scheme outlined above (once again, starting from the radial-Earth velocity model). As is clear from Figure 5, the shape and extent of the input structure is reasonably well determined for both *P* and *S* waves. Thus we conclude that the travel time inversion actually requires the presence of high-velocity subducting slab beneath continental South America. Note, however, that the recovered amplitude of the anomalies is reduced by about 50% (the scales of the synthetic and recovered plots are different by a factor of 2). Therefore, we expect that, although the shape of the anomalies that we recover from the real data should be reasonably reliable, the amplitudes are likely to have been underestimated significantly.

[16] In Figure 6, we demonstrate the ability of the data sets to resolve the lateral extent of the slab at 200 km depth. The top panels show synthetic models with slabs that extend 70 less and 70 km more to the SW on the left and right, respectively. Below these are the recovered anomalies for both the *P* and *S* wave data sets. Once again the "synthetic" data in all cases were determined from 3D ray-tracing through the synthetic models and then the inversions were performed iteratively starting from a radial-Earth velocity model. All other parameters (station terms, earthquake relocations, regularizations weights) remained the same as in the inversion of the real data. These tests show that the lateral extent of the slab is reasonably well resolved by these data sets, even though the amplitudes of the anomalies are once again underestimated (note that the scales of the synthetic and recovered models once again differ by a factor of 2).

6. Slab Overriding and Geodynamic Implications

[17] Because South American continental lithosphere is still clearly attached to oceanic South America subducting along the Lesser Antilles with no discernible relative motion between the two types of plate, we infer that the slab must be free to pivot and rotate, leading to emplacement of its detached portion beneath the continent (Figure 7). South America could not otherwise override its own slab without attendant deformation elsewhere along the continent-ocean passive margin. Thus, the mantle that was beneath northeastern South America from the time of Triassic rifting of North and South America (opening of the Caribbean Basin) must have been mobile enough to flow as it was displaced by the slab now beneath South America. Mantle behind the slab (that is, on its NW, Caribbean side) must also have flowed to fill in behind the slab as it moved. Measurements of shear wave splitting recorded at the SECaSA92 array, which reveal the pattern of mantle deformation beneath the array are consistent with this scenario of mobile mantle and moving slab emplacement beneath the continent [*Russo et al.*, 1996]. An important implication of South America overriding its own detached slab is that both the slab and the continent have significant motion relative to underlying upper mantle: South America is known to move westward between 2 and 3 cm yr^{-1} relative to assumed fixed hot spots [*Minster and Jordan*, 1978; *Gripp and Gordon*, 1990; *Silver et al.*, 1998], and, by inference, relative to the deeper mantle. Since the slab has been overridden by the continent and assumed an ENE-WSW trend from an originally E-W trend, the detached portion of the slab must also be moving, and with a motion differing from continental South America's, relative to the deep mantle (Figure 7). The motion of the detached slab probably has little dynamic effect on the Caribbean plate, which may not be moving relative to the mesosphere [*Jordan*, 1975], but it most likely alters the force balance on both oceanic and continental portions of the South American plate. The latter effect arises as the slab detaches along an east propagating tear, consistent with eastward diachronous development of the plate boundary zone [*Speed*, 1985], and slab pull of the detached portion of slab concentrates stress at the tear [*Yoshioka and Wortel*, 1995], increasing the slab loading on unsubducted continental South America. This loading may explain the obvious topographic differences (Figure 1) between the Serranía (elevated) and the Gulf of

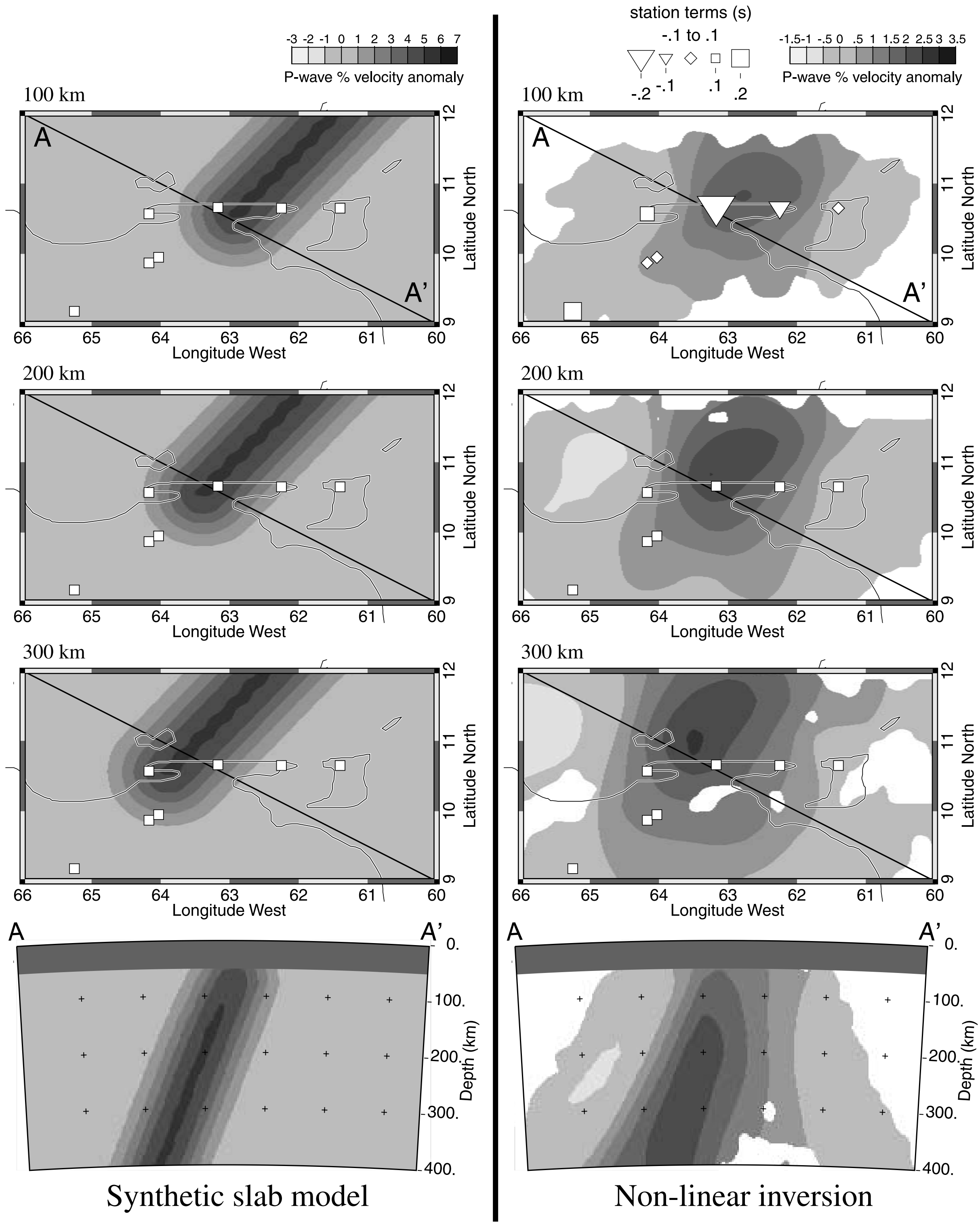

Figure 5. Resolution tests for *P* wave and *S* wave data sets. On the left of each figure: input velocity perturbations (map views at three depths, 100, 200, and 300 km, and cross section along line A-A′). On the right of each figure, map views of the velocity anomalies recovered from inversion of synthetic data from rays with source-receiver geometry of actual data (and with random Gaussian noise of 0.05 s RMS added to the *P* wave and 0.1 s RMS added to the *S* wave synthetic data). Inverted station terms are also shown, topmost figure on right. Note the factor of 2 difference in scales between the synthetic and inversion models, and the close correspondence between resolution test results (right-hand panels) and inversion results of the real data (Figure 4). These tests indicate that the spatial extent of the slab is reasonably well resolved, but that the amplitudes of the anomalies are probably underestimated by about a factor of 2.

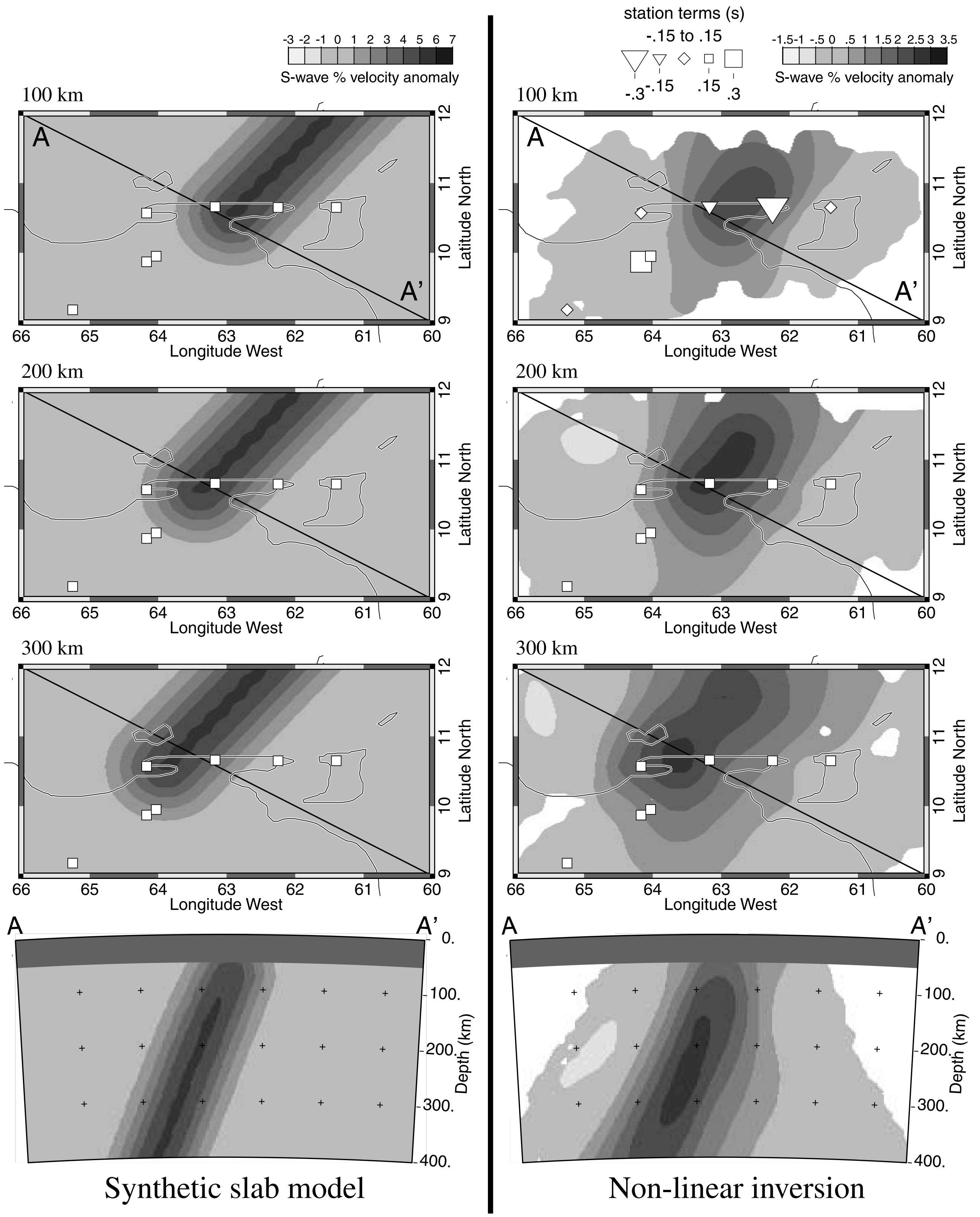

Figure 5. (continued)

Paria (depressed): the slab is currently detaching beneath the Gulf of Paria, and therefore the negative buoyancy of the slab is concentrated there, depressing the continental margin.

[18] Comparison of the locus of slab beneath South America and the high-low paired gravity anomalies discussed above shows clearly that slab, arc platform extension, and the large negative Bouguer anomaly are related. The slab extends SW almost as far as the paired gravity anomalies. The presence of the slab beneath the continent explains the anomaly pair: the load of the slab downwarps the South American continental

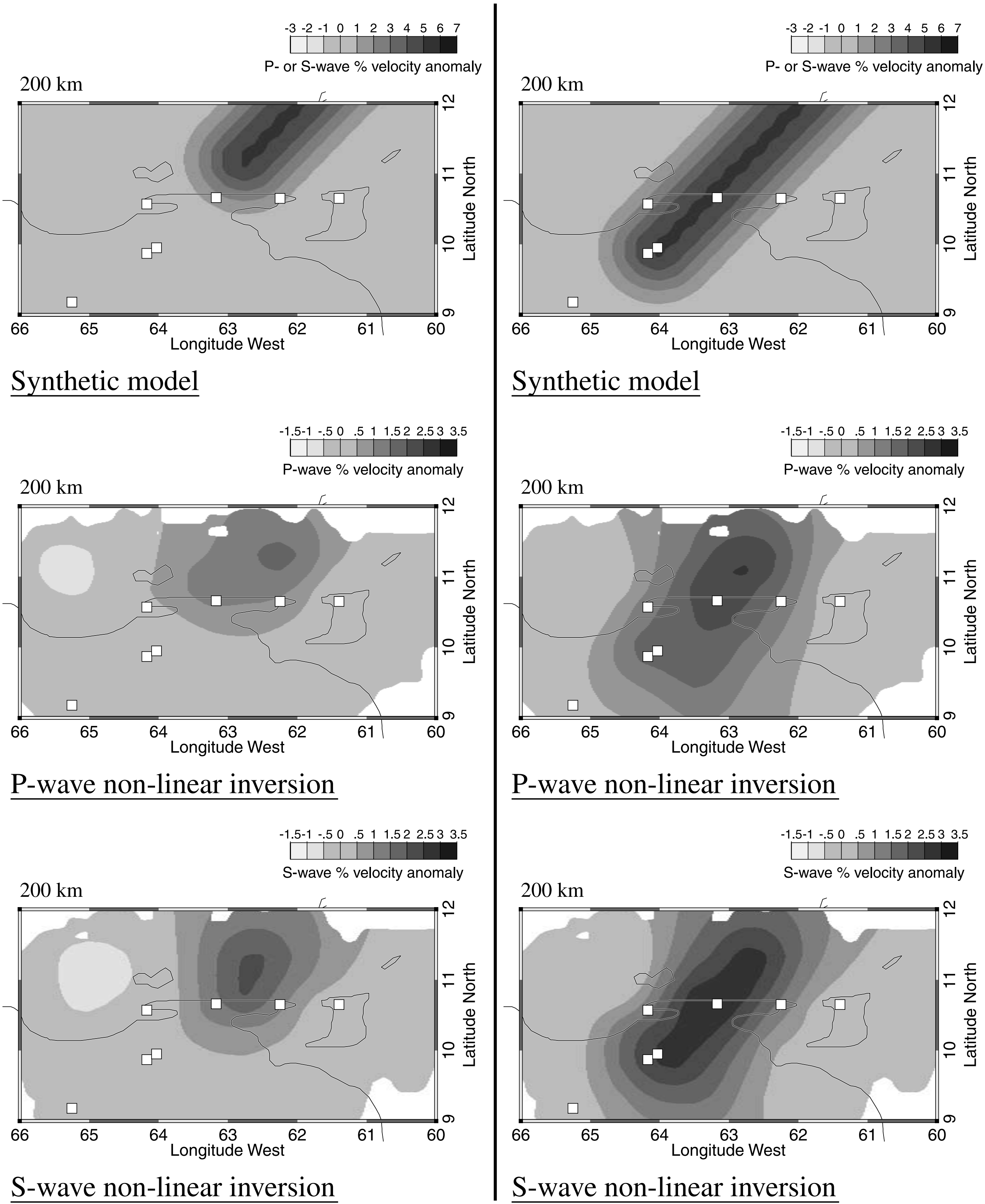

Figure 6. Resolution tests for slabs with lesser and greater along strike extent. Shown are equivalent slices as in Figure 5 except only at 200 km depth. The synthetic data were calculated using ray paths determined by 3-D raytracing though the synthetic models and therefore any biases introduced through the nonlinearity of the inversion scheme (due to ray-bending) should also be reflected in these resolution tests. The inversions were once again performed with the same parameters as with the inversion of the real data.

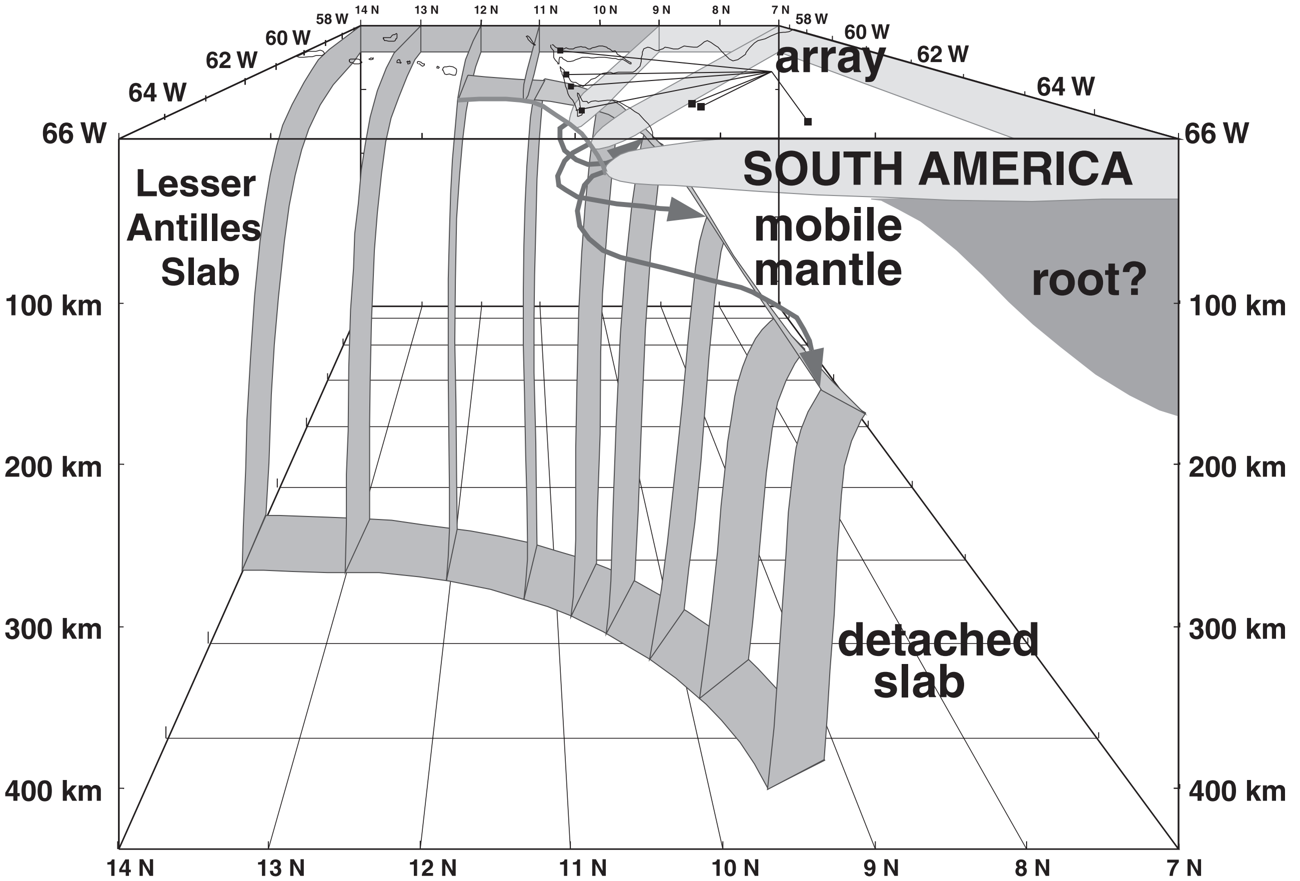

Figure 7. Block diagram of SE Caribbean looking eastward. Thin black lines at surface denote coastlines of South America and Lesser Antilles. Detached and detaching slab shown beneath South America; position of SECaSA92 array stations on surface designated by black squares. Subducted slab detaches just NE of Trinidad; detached, aseismic continuation inferred from high-velocity anomaly lies beneath continental South America. Arrows connect points on detached slab edge to original attachment points on the South American continental margin prior to subduction and detachment. Note that for slab to attain its current position, the mantle beneath the continental South America plate boundary zone must be mobile, e.g., not cratonic. Assuming the Guyana Shield has a cratonic root, it would lie as shown. See color version of this figure at back of this issue.

lithosphere, displacing underlying mantle without formation of high mountains normally associated with such negative Bouguer anomalies (note the Bouguer low is centered on the west coast of the Gulf of Paria, hence at sea level) [*Russo and Speed*, 1992, 1994]. The arc platform extension is not volcanically active perhaps because the continent has wedged beneath the overriding Caribbean plate and because the mantle wedge below the continental plate may have been replaced by sub-Caribbean mantle that flowed in from further west [*Russo and Silver*, 1994; *Russo et al.*, 1996].

7. Conclusions

[19] Inversions of *P* and *S* wave travel time anomalies to the SECaSA92 array in NE Venezuela and Trinidad reveal that subducted oceanic South American lithosphere lies beneath continental South America. This aseismic slab is a southwestern continuation of South American lithosphere subducted along the Lesser Antilles island arc. The slab is attached to continental SA northeast of the Paria Peninsula, but is detached SW of this region. The slab apparently extends to approximately 9°N, 64°W, coincident with the western limit of the east Venezuelan fold and thrust belt. The detached oceanic slab contributes to the unique gravity anomaly low that occurs in this region because it is a subsurface load on the continental lithosphere which depresses continental crust thereby displacing mantle below. The emplacement of oceanic South America slab beneath continental South America developed diachronously, progressing from west to east, during the generally eastward motion of the Caribbean Plate. The presence of the slab beneath the continent indicates that the subcontinental mantle that was displaced by the slab must have been mobile, and that the mantle on the Caribbean (NW) side of the slab is also mobile.

[20] **Acknowledgments.** Many thanks to Randy Kuehnel, without whom this work would not have been possible. Thanks also to Marisabel Munõz, Cenis Teran, and Jose Sgambati for help with servicing stations. Lloyd Lynch, and Joan Latchman were indispensable in establishing the TRNV station. Enrique Gajardo Wolff and Selwyn Sacks played a crucial role in establishing our collaboration. We thank Bob Speed and George Helffrich for edifying discussion. We benefited from helpful reviews by James Kellogg, Bill Spence, Edi Kissling, Dapeng Zhao, and Associate Editors Rob Van der Hilst and Susan Schwartz. We used GMT by *Wessel and Smith* [1991, 1995] to make Figures 1, 2, and 7. This work was supported by NSF

grant EAR 92-19187 to R. M. Russo and D. E. James, and by a Carnegie Institution Fellowship to J. C. VanDecar.

References

Aki, K., and P. G. Richards, *Quantitative Seismology*, 932 pp., W. H. Freeman, New York, 1980.
Avé Lallement, H. G., Transpression, displacement partitioning, and exhumation in the eastern Caribbean/South American plate boundary zone, *Tectonics*, *16*, 272–289, 1997.
Avé Lallement, H. G., and L. R. Guth, Role of extensional tectonics in exhumation of eclogites and blueschists in an oblique subduction setting: Northeastern Venezuela, *Geology*, *18*, 950–953, 1990.
Bladier, Y., Rocas verdes de la región de Carupano, Venezuela, plano de Despaque Corrimientos, *Bol. Geodin. Com. Int. Geodin.*, *2*, 35–49, 1979.
Bonini, W. E., Anomalous crust in the eastern Venezuela Basin and the Bouguer gravity anomaly field of northern Venezuela and the Caribbean borderland, *Geol. Mijnbouw*, *57*, 117–122, 1978.
Bosch, M., *P* wave velocity tomography of the Venezuelan region from local arrival times, *J. Geophys. Res.*, *102*, 5455–5472, 1997.
Bostock, M. G., and J. C. VanDecar, Upper mantle structure of the northern Cascadia subduction, *Can. J. Earth Sci.*, *32*, 1–12, 1995.
Cline, A. K., FITPACK—Software package for curve and surface fitting employing splines under tension, Dept. of Comput. Sci., Univ. of Texas at Austin, 1981.
Constable, S. C., R. L. Parker, and C. G. Constable, Occam's inversion: A practical algorithm for generating smooth models from electromagnetic sounding data, *Geophysics*, *52*, 289–300, 1987.
DeMets, C., R. G. Gordon, D. F. Argus, and S. Stein, Current plate motions, *Geophys. J. Int.*, *101*, 425–478, 1990.
Feo-Codecido, G., F. A. Smith Jr., N. Aboud, and E. de Di Giacomo, Basement and Paleozoic rocks of the Venezuelan Llanos basins, in *The Caribbean-South American Plate Boundary and Regional Tectonics*, *Geol. Soc. America, Mem. 162*, edited by W. E. Bonini, R. B. Hargraves, and R. Shagam, pp. 189–212, Geol. Soc. of Am., Boulder, Colo., 1984.
Foland, K. A., R. C. Speed, and J. Weber, Geochronologic studies of the hinterland of the Caribbean mountains orogen of Venezuela and Trinidad, *Geol. Soc. Am., Abstr. Programs*, *24*, A148, 1992.
Grand, S. P., Mantle shear structure beneath the Americas and surrounding oceans, *J. Geophys. Res.*, *99*, 11,591–11,621, 1994.
Gripp, A. E., and R. G. Gordon, Current plate velocities relative to the hotspots incorporating the NUVEL-1 global plate motion model, *Geophys. Res. Lett.*, *17*, 1109–1112, 1990.
Huber, P. J., *Robust Statistics*, 320 pp., John Wiley, New York, 1981.
Jordan, T. H., The present-day motions of the Caribbean plate, *J. Geophys. Res.*, *80*, 4433–4439, 1975.
Jordan, T. H., and W. S. Lynn, A velocity anomaly in the lower mantle, *J. Geophys. Res.*, *79*, 2679–2685, 1974.
Kendall, J.-M., and P. G. Silver, Constraints from seismic anisotropy on the nature of the lowermost mantle, *Nature*, *381*, 409–412, 1996.
Kennett, B. L. N., and E. R. Engdahl, Travel times for global earthquake location and phase identification, *Geophys. J. Int.*, *105*, 429–465, 1991.
Lay, T., Localized velocity anomalies in the lower mantle, *Geophys. J. R. Astron. Soc.*, *72*, 483–516, 1983.
Metz, H. L., Geology of the El Pilar Fault Zone, State of Sucre, Venezuela, *Trans. Carib. Geol. Conf., 4th*, 193–198, 1968.
Minster, J. B., and T. H. Jordan, Present-day plate motions, *J. Geophys. Res.*, *83*, 5331–5354, 1978.
Molnar, P., and L. Sykes, Tectonics of the Caribbean and Middle America regions from focal mechanisms and seismicity, *Geol. Soc. Am. Bull.*, *80*, 1639–1684, 1969.
Neele, F., J. C. VanDecar, and R. Snieder, A formalism for including amplitude data in tomographic inversions, *Geophys. J. Int.*, *115*, 482–496, 1993a.
Neele, F., J. C. VanDecar, and R. Snieder, The use of *P* wave amplitude data in a joint tomographic inversion with travel times for upper mantle velocity structure, *J. Geophys. Res.*, *98*, 12,033–12,054, 1993b.
Parker, R. L., *Geophysical Inverse Theory*, 386 pp., Princeton Univ. Press, Princeton, N. J., 1994.
Parnaud, F., Y. Gou, J.-C. Pascual, I. Truskowski, O. Gallango, H. Passalacqua, and F. Roure, Petroleum geology of the central part of the eastern Venezuelan Basin, in *Petroleum Basins of South America*, edited by A. J. Tankard et al., *AAPG Mem.*, *62*, 741–756, 1995.
Passalacqua, H., F. Fernandez, Y. Gou, and F. Roure, Crustal architecture and train partitioning in the eastern Venezuelan ranges, in *Petroleum Basins of South America*, edited by A. J. Tankard et al., *AAPG Mem. 62*, 667–679, 1995.
Perez, O. J., and Y. P. Aggarwal, Present-day tectonics of the southeastern Caribbean and northeastern Venezuela, *J. Geophys. Res.*, *86*, 10,791–10,804, 1981.
Rossi, T., J.-F. Stephan, R. Blanchet, and G. Hernandez, Étude géologique de la Serranía del Interior Oriental (Venezuela) sur le transect Cariaco-Maturin, *Rev. Inst. Fr. Pet.*, *42*, 3–30, 1987.
Roure, F., J. O. Carnevali, Y. Gou, and T. Subieta, Geometry and kinematics of the north Monagas thrust belt (Venezuela), *Mar. Pet. Geol.*, *11*, 347–362, 1994.
Russo, R. M., and P. G. Silver, Trench-parallel flow beneath the Nazca plate from seismic anisotropy, *Science*, *263*, 1105–1111, 1994.
Russo, R. M., and R. C. Speed, Oblique collision and tectonic wedging of the South American continent and Caribbean terranes, *Geology*, *20*, 447–450, 1992.
Russo, R. M., and R. C. Speed, Spectral analysis of gravity anomalies and the architecture of tectonic wedging, NE Venezuela and Trinidad, *Tectonics*, *13*, 613–622, 1994.
Russo, R. M., E. A. Okal, and K. C. Rowley, Historical seismicity of the southeastern Caribbean and tectonic implications, *Pure Appl. Geophys.*, *139*, 87–120, 1992.
Russo, R. M., R. C. Speed, E. A. Okal, J. B. Shepherd, and K. C. Rowley, Seismicity and tectonics of the southeastern Caribbean, *J. Geophys. Res.*, *98*, 14,299–14,319, 1993.
Russo, R. M., P. G. Silver, M. Franke, W. B. Ambeh, and D. E. James, Shear-wave splitting in northeast Venezuela, Trinidad, and the eastern Caribbean, *Phys. Earth Planet. Inter.*, *95*, 251–275, 1996.
Salvador, A., and R. M. Stainforth, Clues in Venezuela to the geology of Trinidad and vice-versa, in *Trans. Fourth Carib. Geol. Conf., Trinidad, 1985*, edited by J. B. Saunders, pp. 31–40, Caribbean Printers, Arima, Trinidad & Tobago, 1968.
Schubert, C., Metamorphic rocks of the Araya Peninsula, eastern Venezuela, *Geol. Rundsch.*, *60*, 1571–1600, 1971.
Silver, P. G., R. M. Russo, and C. Lithgow-Bertelloni, The coupling of South American and African plate motion and plate deformation, *Science*, *279*, 60–63, 1998.
Smith, W. H. F., and D. T. Sandwell, Global sea floor tomography from satellite altimetry and ship depth soundings, *Science*, *277*, 1962–1965, 1997.
Speed, R. C., Cenozoic collision of the Lesser Antilles Arc and continental South America and the origin of the El Pilar Fault, *Tectonics*, *4*, 41–69, 1985.
Speed, R. C., G. K. Westbrook, B. Biju-Duval, J. W. Ladd, A. Mascle, J. C. Moore, J. B. Saunders, J. E. Schoonmaker, and S. Stein, *Atlas 10, Ocean Margin Drilling Program, Lesser Antilles and Adjacent Ocean Floor*, Marine Science International, Woods Hole, Mass., 1984.
VanDecar, J. C., and R. S. Crosson, Determination of teleseismic relative phase arrival times using multi-channel cross-correlation and least squares, *Bull. Seismol. Soc. Am.*, *80*, 150–169, 1990.
VanDecar, J. C., and R. Snieder, Obtaining smooth solutions to large, linear, inverse problems, *Geophysics*, *59*, 818–829, 1994.
Van der Hilst, R. D., Tomography with P, PP and pP delay-time data and the three-dimensional mantle structure below the Caribbean region, Ph.D. thesis, 250 pp., Univ. of Utrecht, 1990.
Van der Hilst, R. D., and P. Mann, Tectonic implications of tomographic images of subducted lithosphere beneath northwestern South America, *Geology*, *22*, 451–454, 1994.
Van der Hilst, R. D., and W. Spakman, Importance of reference model in linearized tomography and images of subduction below the Caribbean plate, *Geophys. Res. Lett.*, *16*, 1093–1096, 1989.
Wadge, G., and J. B. Shepherd, Segmentation of the Lesser Antilles subduction zone, *Earth Planet. Sci. Lett.*, *71*, 297–304, 1984.
Wessel, P., and W. H. F. Smith, Free software helps map and display data, *Eos Trans. AGU*, *72*, 441–446, 1991.
Wessel, P., and W. H. F. Smith, New version of the Generic Mapping Tools released, *Eos Trans. AGU*, *76*, 329, 1995 [version 3.0]
Yoshioka, S., and M. J. R. Wortel, Three-dimensional numerical modeling of detachment of subducted lithosphere, *J. Geophys. Res.*, *100*, 20,223–20,244, 1995.
Ysaccis, R., and A. W. Bally, Cariaco and Carúpano basins, (Abstract), paper presented at *SE Caribbean Plate Boundary Zone Workshop*, Rice University, Oct. 3 to Oct. 4, 1997.

W. B. Ambeh, Seismic Research Unit, University of the West Indies, St. Augustine, Trinidad, Trinidad and Tobago.
M. Franke, Kinemetrics, Inc., 222 Vista Avenue, Pasadena, CA 91107, USA.
D. E. James and J. C. VanDecar, Department of Terrestrial Magnetism, Carnegie Institution of Washington, 5251 Broad Branch Rd., N.W., Washington, D. C. 20015, USA. (vandecar@dtm.ciw.edu)
R. M. Russo, Department of Geological Sciences, Northwestern University, Evanston, IL 60208, USA. (ray@earth.nwu.edu)

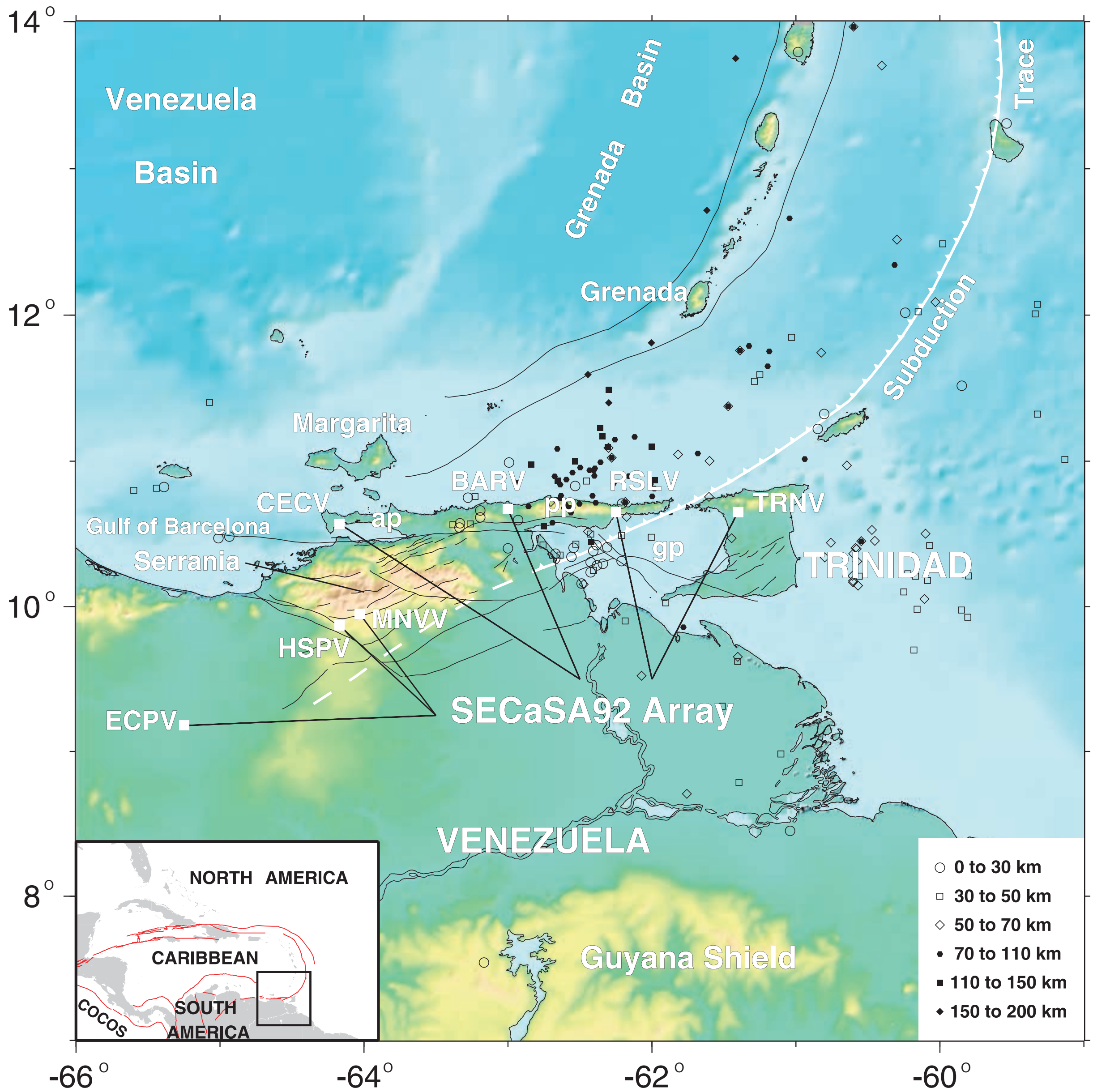

Figure 1. Map of study region. Coastlines (black) overlain on 2-min bathymetry [*Smith and Sandwell*, 1997] and topography (30-s NGDC). Boundaries of Lesser Antilles arc platform shown in black; lithospheric subduction trace is heavy white line, teeth on overriding side. Faults of the foreland region also shown (thin black lines). SECaSA92 station locations are white squares. Filled and unfilled black symbols are NEIC seismicity 1963–1993, 20 or more recording stations. Geographic place names: ap, Araya Peninsula; pp, Paria Peninsula; gp, Gulf of Paria; Serranía, Serranía del Interior.

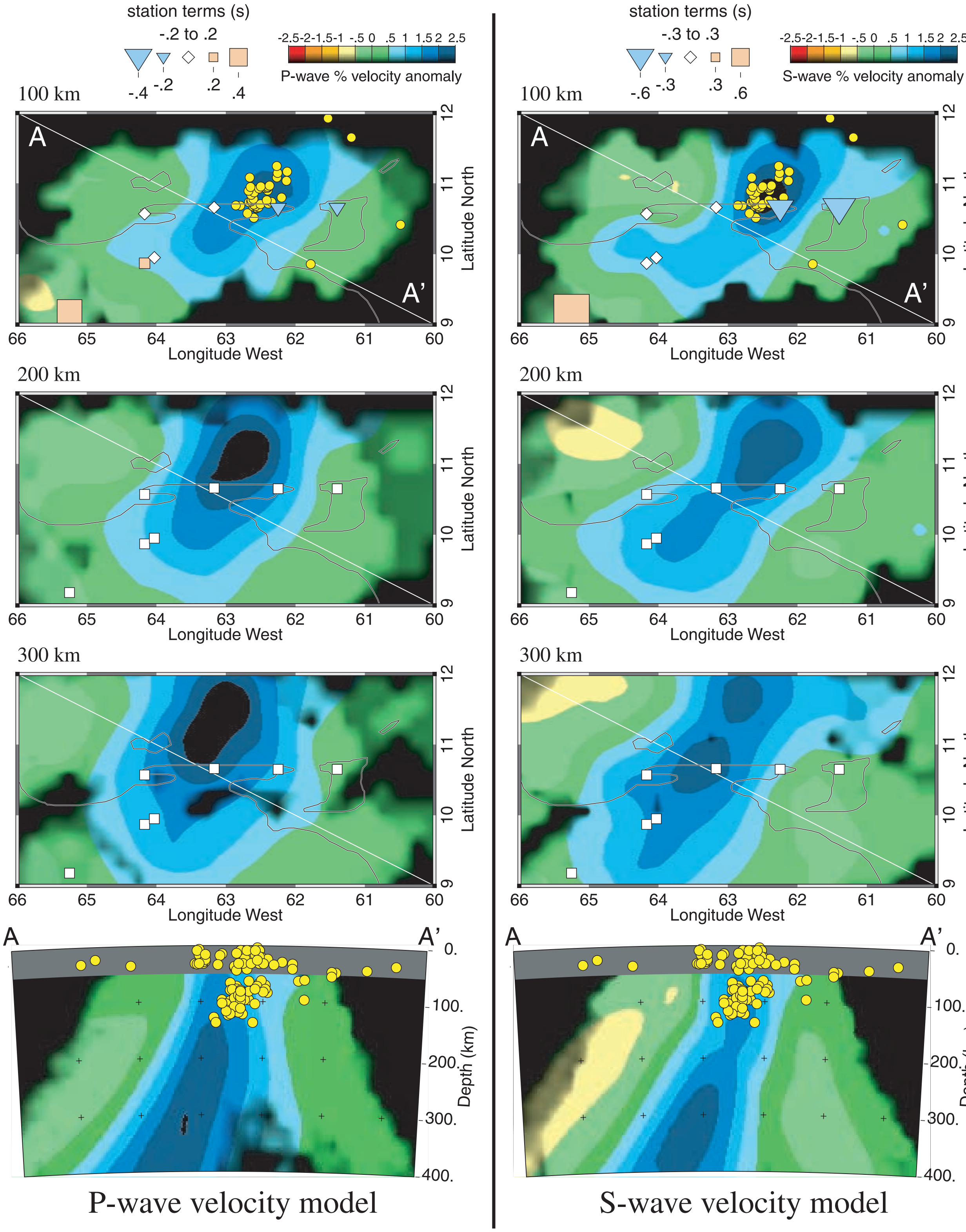

Figure 4. Horizontal sections through *P* wave (left) and *S* wave (right) velocity percent perturbation models (slowness, 1/velocity, was actually determined in the inversion) at constant depths of 100, 200 and 300 km; vertical cross sections (bottom) at locations shown by white lines in top three sections. Perturbations are with respect to global radial-Earth velocity model IASP91 [*Kennett and Engdahl*, 1991]. Yellow dots: earthquakes within ±30 km of each depth section. Note tabular high-velocity anomaly coincident with Paria slab earthquakes but extending SW from Paria beneath SA. We interpret this anomaly as both the seismically active and aseismic slab continuation beneath SA.

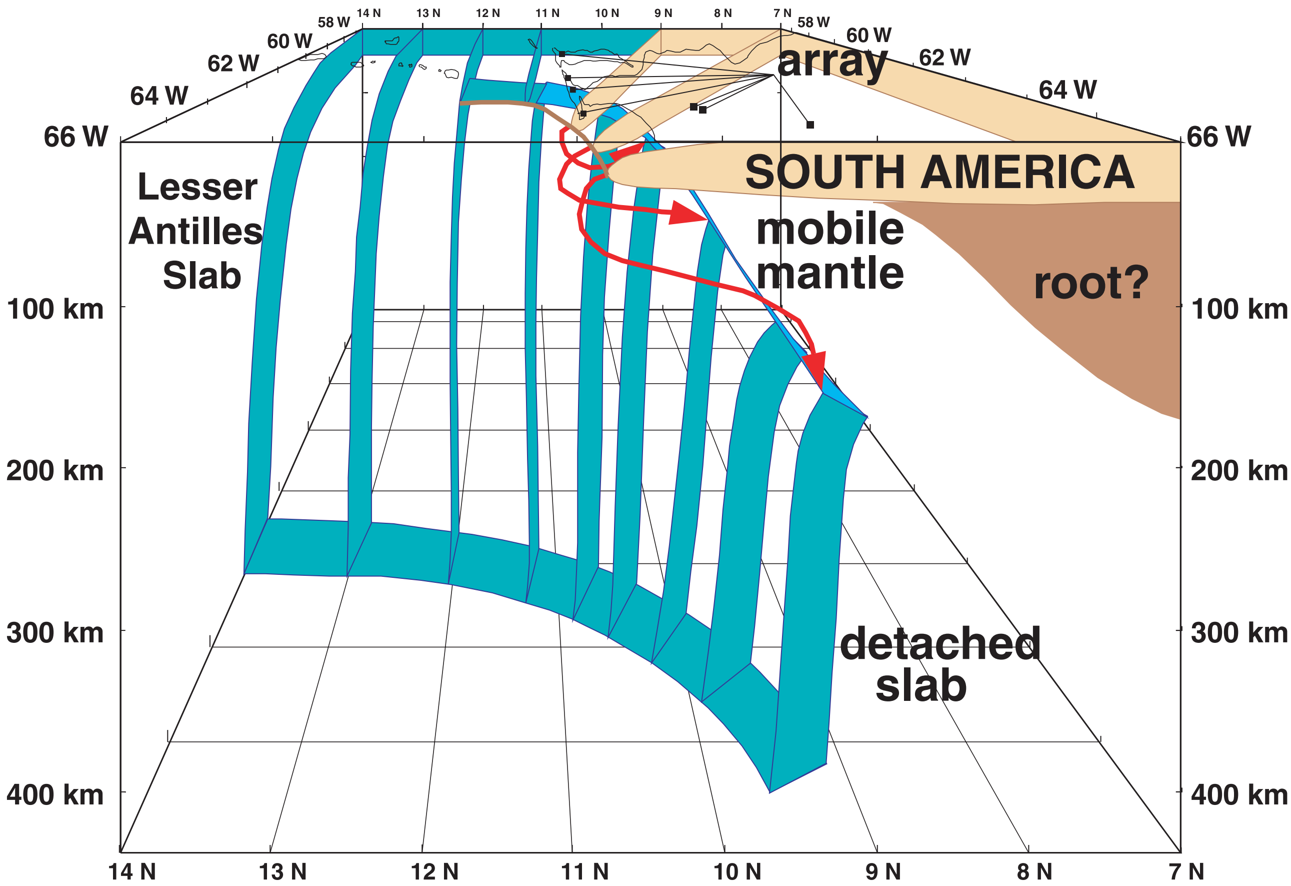

Figure 7. Block diagram of SE Caribbean looking eastward. Thin black lines at surface denote coastlines of South America and Lesser Antilles. Detached and detaching slab shown beneath South America; position of SECaSA92 array stations on surface designated by black squares. Subducted slab detaches just NE of Trinidad; detached, aseismic continuation inferred from high-velocity anomaly lies beneath continental South America. Arrows connect points on detached slab edge to original attachment points on the South American continental margin prior to subduction and detachment. Note that for slab to attain its current position, the mantle beneath the continental South America plate boundary zone must be mobile, e.g., not cratonic. Assuming the Guyana Shield has a cratonic root, it would lie as shown.